MATEC Web of Conferences **321**, 12027 (2020) https://doi.org/10.1051/matecconf/202032112027
The 14th World Conference on Titanium

Evolution of distance between ω particles in metastable β-Ti alloy determined from in-situ small angle neutron scattering

Pavel Zháňal[1,2,*], *Vasyl* Ryukhtin[3], *Gergely* Farkas[1,3], *Peter* Kadletz[3,4], *Uwe* Keiderling[4], *Dirk* Wallacher[4], and *Petr* Harcuba[1]

[1]Department of Physics of Materials, Charles University, Prague, Czech Republic
[2]Material and Mechanical Properties, Research Centre Rez Ltd., Rez, Czech Republic
[3]Nuclear Physics Institute, The Czech Academy of Sciences, Rez, Czech Republic
[4]Helmholtz-Zentrum Berlin für Materialien und Energie, Berlin, Germany

Abstract. The evolution of distance between ω particles in metastable β Ti-15Mo alloy (8.1 in at. %) was determined from in-situ small angle neutron scattering (SANS). SANS data were recorded during heating of the material from room temperature to 600 °C with the heating rate of 1 °C/min. The results agree with previously determined ordering of ω particles in a cubic three-dimensional array with the axes along the cubic axes $\langle 100 \rangle_\beta$ of the host lattice. The distance between particles, which increases with temperature, was investigated in three orientations with the incident beam parallel to $[100]_\beta$, $[110]_\beta$ and $[111]_\beta$.

1 Introduction

Titanium alloys have high strength, low density, and excellent corrosion resistance, which make them attractive for a variety of applications [1]. Properties required for aerospace are high strength, low density and good creep resistance up to about 550 °C. Biomedicine and chemical industry appreciate corrosion resistance and high strength of these alloys. Wider use in automotive applications has been hindered by a relatively high cost of titanium [2]. The high cost of titanium alloys can be compensated by fully exploiting their outstanding functional properties compared to other materials [3]. Therefore, optimization of mechanical properties of titanium alloys is of primary importance and it can be achieved only through a complex understanding of mechanisms of phase transformations occurring in these materials.

According to the type and amount of alloying elements and the resulting phase composition, titanium alloys are commonly classified as α, $\alpha + \beta$, metastable β and stable β [1]. Metastable β alloy is defined as a titanium alloy with sufficient β-stabilizer content to suppress $\beta \rightarrow \alpha'$ or α'' martensitic transformation during quenching to room temperature. In many metastable β alloys, β phase undergoes a partial transformation upon quenching to the so-called athermal ω phase (ω_{ath}) [4, 5], which forms as homogeneous dispersion of extremely fine particles (size 1-4 nm) [5]. $\beta \rightarrow \omega$ transformation involves a displacement in the $\langle 111 \rangle$ direction of β lattice [6]. ω_{ath} has a hexagonal symmetry [7] and forms a coherent interface with β phase. The structure of this interface can be characterized as an elastically

*e-mail: pavel.zh@karlov.mff.cuni.cz

distorted bcc lattice [1]. Upon annealing in the $\beta + \omega$ phase field (at temperatures 200 – 400 °C, depending on alloy composition), ω phase grows to form the so-called isothermal ω phase, which retains the same crystallographic symmetry as ω_{ath} [1].

ω_{iso} phase is stabilized by an irreversible diffusion-controlled rejection of β stabilizing elements from ω_{iso} particles. ω_{iso} particles typically coarsen during annealing and are weakly ordered in a cubic array along $\langle 100 \rangle_\beta$ directions [8].

2 Materials and methods

2.1 Material

In this research a single crystals of metastable β-titanium alloy Ti-15Mo (8.1 at. % of Mo) were studied. This alloy is used mainly for biomedical applications. It was originally developed for the chemical industry to provide a titanium alloy with improved corrosion resistance, low elastic modulus, high strength, good fatigue resistance, and good ductility. High temperature applications were also investigated but thermal handling difficulties and microstructure instability at moderate temperatures prevented the extended use in the aerospace industry [9].

2.1.1 Preparation of single crystals

The diffraction experiments were performed on single-crystalline Ti-15Mo. The single crystals were grown in the optical furnace from a rod with diameter of 9 mm. The furnace was evacuated by a turbomolecular pump up to 10^{-6} mbar to avoid oxidation of the titanium alloy. After proper evacuation the quartz chamber was filled with high purity Ar protective atmosphere. At the beginning of each crystal growth, a neck was created in order to isolate one grain. The pulling rate was 10 mm/h and the rotation velocity of both the upper and the lower shaft was 5 rpm. The total length of grown crystals was up to 9 cm. A thorough explanation of the growth process can be found in [10].

2.2 Electrical resistance

Measurements of electrical resistance of the samples were performed employing a self-made apparatus. A four-point methods of electrical resistance measurement was employed. The scheme of electrical circuit of this technique is shown in Fig. 1a. Due to the setup of this method, the resistance of contact leads and their welds with the sample does not affect the measured electrical resistance. The current is the same at all points in the circuit. As only voltage drop across the sample is measured (and not the wires resistances), the calculated electrical resistance represents solely the resistance of the sample (R_{sample}). The numbers 1 - 4 in Fig. 1a label wires, which were welded to respective contacts on the sample (see Fig. 1b).

The voltage was measured simultaneously with the electrical current utilizing nanovoltmeter Keithley 2182 and SourceMeter Keithley 2400 device, respectively, which allows relative measuring error to be less than 10^{-4} at each measured point while acquiring about 2 points per second [11]. There are two heating elements placed on top and underneath the sample, respectively. Each heating coil has its own source (Kikusui PAS-40-18), which provide current used for heating. The temperature is measured by K type thermocouple placed in a vicinity of the sample. Measured samples were flat of the thickness slightly less than 1 mm and the size of 15×10 mm^2. They were cut to the shape of letter S to increase the effective length of the sample for electric current flow and four contacts were appropriately joined. The samples shape and dimensions are shown in Fig. 1b.

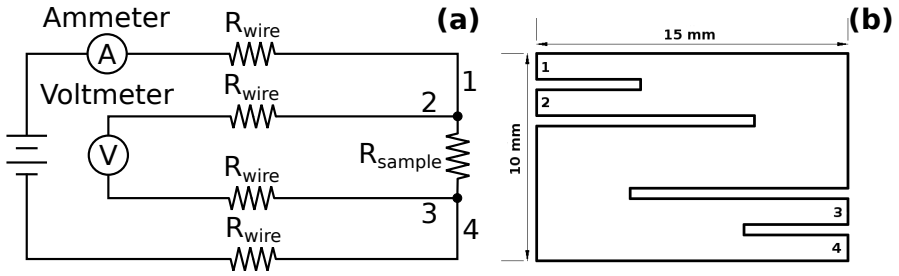

Figure 1: Scheme of: (a) four-point method; (b) the sample shape used for electrical resistance measurements.

2.3 Small angle neutron scattering

Small angle neutron scattering (SANS) experiments were measured at three orientations of the single crystal sample $(111)_\beta$, $(110)_\beta$ and $(100)_\beta$ of β phase with corresponding plane perpendicular to incident neutron beam direction. Samples were installed in vacuum high temperature furnace and one by one heated with the heating rate of 1 °C/min from room temperature up to 600 celsius. SANS experiments were performed at the Helmholtz-Zentrum Berlin (HZB), Germany, at the instrument V4 [12, 13]. Neutrons were recorded on a two-dimensional (2D) gas detector of 128×128 pixels of 5×5 mm^2 in so-called list-mode and afterwards binned by time frames of 5 minutes, which corresponds to temperature range of 5 celsius. The sample-to-detector distance was set to 15.8 m, collimation to 12 m and the wavelength was kept at (5 ± 0.5) Å. The measured data were calibrated using water and corrected by standard measurements of cadmium background. Scattering of the sample in high temperature furnace was used as "buffer" background. Sketch of the V4 instrument can be found in [14].

3 Results and discussion

3.1 Electrical resistance measurements

It was shown that phase transitions in Ti alloys can be detected by means of electrical resistance measurement that is particularly sensitive to evolution of ω phase particles [15–28]. Fig. 2 shows the evolution of normalized electrical resistance (R/R_{20}) of Ti-15Mo alloy during heating with the heating rate of 1 °C/min, where R_{20} is the electrical resistance of the sample either at 20 °C.

The evolution of resistance in metastable β Ti-15Mo alloy exhibits two significant drops due to ongoing phase transformations. The first decrease of the electrical resistance between room temperature and 200 °C is attributed to dissolution of ω_{ath} [19, 21, 23, 29]. Further heating results in increase of the electrical resistance, which is caused by increasing electron-phonon scattering coupled with formation of ω_{iso} [29]. The second decline of the electrical resistance (between 335 °C and 560 °C) by further coarsening of ω particles coupled with decrease of volume fraction of ω phase [30]. During heating above 560 °C, the resistance increases and the concentration of α phase first increases to reach an equilibrium and than close to β-transus decreases again. Above the β-transus (about 730 °C - note a small change of slope of the curve in Fig. 2 at this temperature) α phase dissolves completely.

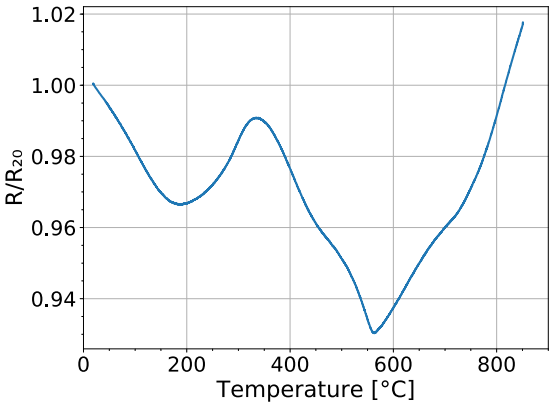

Figure 2: The evolution of normalized resistance of metastable β Ti-15Mo alloy.

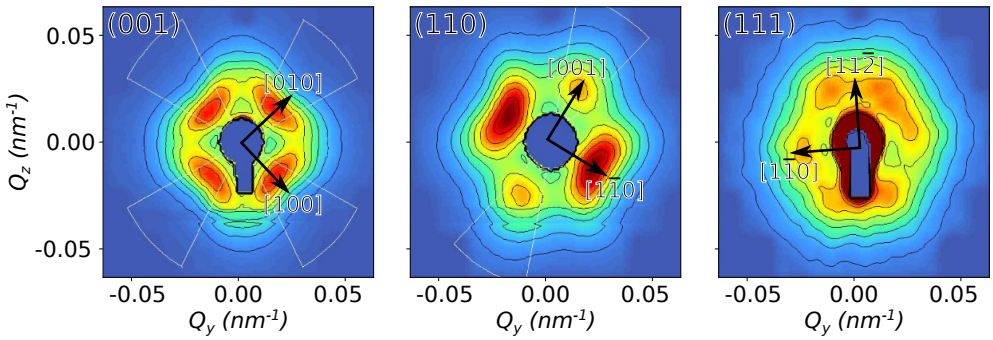

Figure 3: The SANS maps of the samples heated to about 500 °C measured in three orientations of the primary neutron beam. The arrows denote the crystallographic directions in β host lattice.

3.2 SANS

In this study we investigated Ti-15Mo single crystals in three orientations of primary beam with respect to β matrix. The SANS diffraction patterns of these samples with the incident beam perpendicular to $(100)_\beta$, $(110)_\beta$ and $(111)_\beta$ is shown in Fig. 3. The results confirm the spatial ordering of ω particles in a cubic three-dimensional array with the axes along the cubic axes $\langle 100\rangle_\beta$ of the β matrix determined from small angle X-ray scattering [8].

The $[100]_\beta$ orientation of the primary beam, shows fourfold symmetry and there were detected four quasi-peaks in the directions [010] and [001]. On the other hand, twofold symmetry was observed for the $[110]_\beta$ orientation of the primary beam. There are two peaks at $[001]_\beta$ direction and two quasi-peaks lying along the $[1\bar{1}0]_\beta$. A sixfold symmetry is observable in the $[111]_\beta$ orientation of the primary beam. Peaks in this orientation are less distinct compared to ones in other orientations due to lower overall intensity caused by larger dimensions of the sample in this direction, therefore larger interactions of neutrons with matter. The shape of quasi-peaks is caused by distribution of wavelengths and of positions of ω particles.

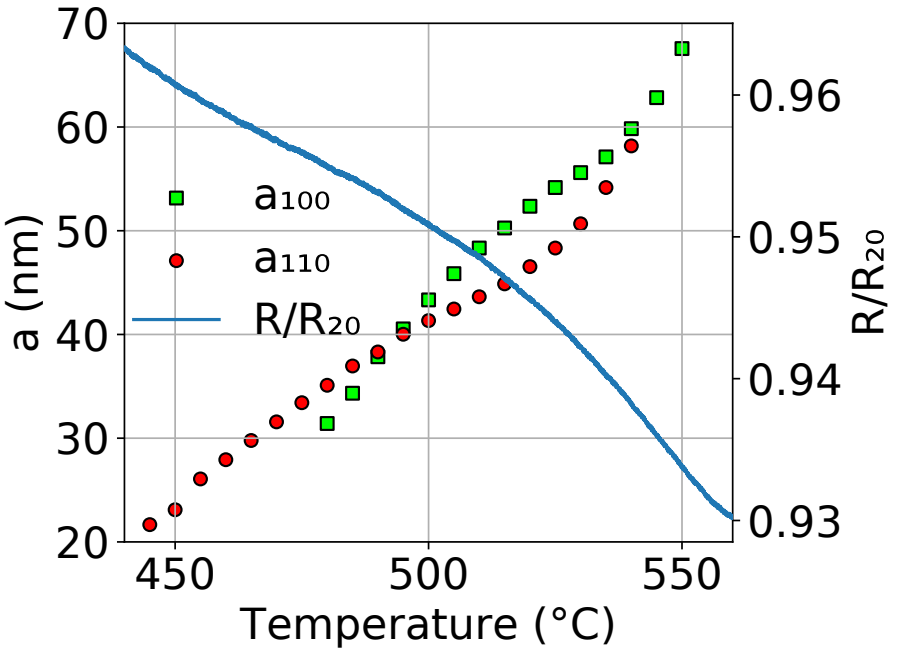

Figure 4: Comparison of the evolutions of distances of ω particles determined from the experiments with $[100]_\beta$ and $[110]_\beta$ orientations of the primary beam and normalized electrical resistance. The subscripts of lattice parameter label the orientation from which the parameter was determined.

The evolution of the lattice parameter of a cubic three-dimensional array of ω particles, which was determined from the SANS diffraction patterns measured in-situ during heating with heating rate of 1 °C/min is shown in Fig. 4. The values are presented only in the temperature interval of 445 °C - 550 °C. Bellow this temperature, ω particles were too close to each other and the peaks corresponding to these distances were outside of the detector. With the increasing temperature the diffraction maxima approached center of the detector and at temperatures above 550 °C hid behind the beamstop and subsequently disappeared due to dissolution of ω phase at 560 °C [28, 30].

The lattice parameters were determined by fitting position of peaks in regions highlighted by white line in Fig. 3 (along $\langle 100 \rangle_\beta$) for the $[100]_\beta$ and $[110]_\beta$ orientations of the primary beam (for $[100]_\beta$ quasi-peaks were fitted, since no clear peaks can be observed in this orientation). Due to low intensity of the peaks in the $[111]_\beta$ orientation of the primary beam, lattice parameters were not determined in this case.

The decrease of electrical resistance in the temperature interval of 445 °C - 550 °C is accompanied by coarsening of ω particles, which have size about 15 nm at 420 °C (see Fig. 5) and about 50 nm at 550 °C [28]. The coarsening is accompanied by an increase of the distance between ω particles. The lattice parameter of the cubic three-dimensional array of ω particles is approximately equal to their size. The lattice parameter determined from

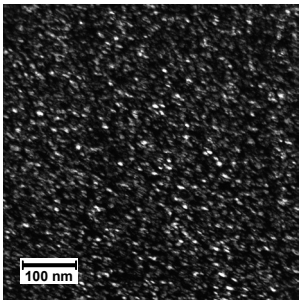

Figure 5: Microstructure of the specimen quenched from 420 °C.

different orientations are nearly equal. The small difference is probably due to complicated fitting of broad (quasi) peaks.

4 Summary

We have studied evolution of positions of ω particles with respect to each other in single crystals of metastable β titanium alloy Ti-15Mo by SANS. We determined the particles distance during heating and confirmed that the particles order in a cubic three-dimensional array with the axes along the cubic axes $\langle 100 \rangle_\beta$ of β matrix.

Acknowledgements

This work was financially supported by the Czech Science Foundation under the project 16-12598S. Pavel Zháňal would like to express gratitude for financial support by the Ministry of Education, Youth and Sport Czech Republic - project LQ1603 Research for SUSEN and to the SUSEN Project (established in the framework of the European Regional Development Fund (ERDF) in project CZ.1.05/2.1.00/03.0108 and of the European Structural and Investment Funds (ESIF) in the project CZ.02.1.01/0.0/0.0/15_008/0000293).

References

[1] G. Lütjering, J.C. Williams, *Titanium*, Engineering Materials, Processes (Springer Berlin Heidelberg, 2007), ISBN 978-3-540-71397-5

[2] C. Leyens, M. Peters, eds., *Titanium and titanium alloys: fundamentals and applications* (Wiley-VCH; John Wiley, 2003), ISBN 978-3-527-30534-6

[3] M. Donachie, *Titanium: A Technical Guide* (AMS International, 1988), ISBN 0-87170-309-2

[4] S.K. Sikka, Y.K. Vohra, R. Chidambaram, Progress in Materials Science **27**, 245 (1982)

[5] S. Banerjee, P. Mukhopadhyay, *Phase transformations: examples from titanium and zirconium alloys*, Number 12 in Pergamon materials series (Elsevier/Pergamon, 2007), ISBN 978-0-08-042145-2

[6] B.S. Hickman, Journal of Materials Science **4**, 554 (1969)

[7] J.M. Silcock, Acta Metall **6**, 481 (1958)

[8] J. Šmilauerová, P. Harcuba, J. Stráský, J. Stráská, M. Janeček, J. Pospíšil, R. Kužel, T. Brunátová, V. Holý, J. Ilavský, Acta Materialia **81**, 71–82 (2014)

[9] J. Disegi, *Implant Materials. Wrought Titanium –15% Molybdenum* (Synthes, 2009)
[10] J. Šmilauerová, J. Pospíšil, P. Harcuba, V. Holý, M. Janeček, Journal of Crystal Growth **405**, 92–96 (2014)
[11] M. Hájek, J. Veselý, M. Cieslar, Materials Science and Engineering: A **462**, 339–342 (2007)
[12] U. Keiderling, A. Wiedenmann, Physica B: Condensed Matter **213–214**, 895–897 (1995)
[13] U. Keiderling, C. Jafta, Journal of large-scale research facilities JLSRF **2**, 97 (2016)
[14] A. Wiedenmann, *Magnetic and Crystalline Nanostructures in FFs as Probed by Small Angle Neutron Scattering* (2008), pp. 33–58
[15] S. Yoshida, Y. Tsuya, J. Phys. Soc. Jpn. **11**, 1206 (1956)
[16] T.S. Luhman, R. Taggart, D.H. Polonis, Scripta Metallurgica **2**, 169 (1968)
[17] J.C. Ho, E.W. Collings, Physical Review B **6**, 3727 (1972)
[18] M.A. Hill, D.H. Polonis, Journal of Materials Science **22**, 2181–2184 (1987)
[19] M. Ikeda, S. Komatsu, T. Sugimoto, K. Kamei, *Negative Temperature Dependence of Resistivity in Ti-Mo Binary Alloys*, in *Proc. 6th Conf. on Ti* (Societe de France Met., 1988), pp. 313–318
[20] F. Prima, J. Debuigne, M. Boliveau, D. Ansel, Journal of materials science letters **19**, 2219 (2000)
[21] T. Gloriant, G. Texier, F. Sun, I. Thibon, F. Prima, J. Soubeyroux, Scripta Materialia **58**, 271 (2008)
[22] F. Bruneseaux, E. Aeby-Gautier, G. Geandier, J. Da Costa Teixeira, B. Appolaire, P. Weisbecker, A. Mauro, Materials Science and Engineering: A **476**, 60–68 (2008)
[23] P. Zháňal, P. Harcuba, J. Šmilauerová, J. Stráský, M. Janeček, B. Smola, M. Hájek, Acta Physica Polonica A **128**, 779 (2015)
[24] P. Zháňal, P. Harcuba, M. Janeček, J. Smilauerová, J. Veselý, B. Smola, M. Zimina, *Phase Transformations in Metastable Ti-15Mo During Linear Heating*, in *Proceedings of the 13th World Conference on Titanium*, edited by V. Venkatesh et al. (TMS (The Minerals, Metals & Materials Society), 2016), pp. 431–436
[25] P. Harcuba, J. Šmilauerová, M. Hájek, P. Zháňal, J. Čapek, *Phase Transformations in Beta-Ti Alloys Studied by In-Situ Methods*, in *Proceedings of the 13th World Conference on Titanium*, edited by V. Venkatesh et al. (John Wiley & Sons, Inc., 2016), p. 437–441, ISBN 978-1-119-29612-6
[26] P. Zháňal, P. Harcuba, M. Hájek, J. Šmilauerová, J. Veselý, M. Janeček, Materials Science Forum **879**, 2318–2323 (2017)
[27] K. Václavová, J. Stráský, P. Zháňal, J. Veselý, V. Polyakova, I. Semenova, M. Janeček, IOP Conference Series: Materials Science and Engineering **194**, 012021 (2017)
[28] P. Zháňal, P. Harcuba, M. Hájek, B. Smola, J. Stráský, J. Šmilauerová, J. Veselý, M. Janeček, Journal of Materials Science **53**, 837–845 (2018)
[29] T. Gloriant, G. Texier, F. Prima, D. Laillé, D.M. Gordin, I. Thibon, D. Ansel, Advanced Engineering Materials **8**, 961–965 (2006)
[30] P. Zháňal, P. Harcuba, M. Hájek, J. Šmilauerová, J. Veselý, L. Horák, M. Janeček, V. Holý (2019), Manuscript submitted for publication